

Figure 1 : Schematic representation of Photo-CREC-Air and its associated internal components.

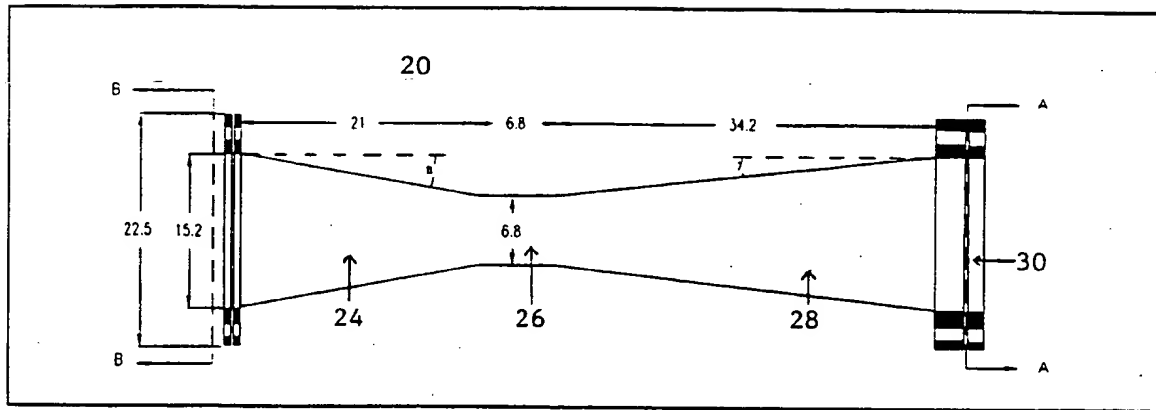


Figure 2 : Schematic representation of the Venturi section.

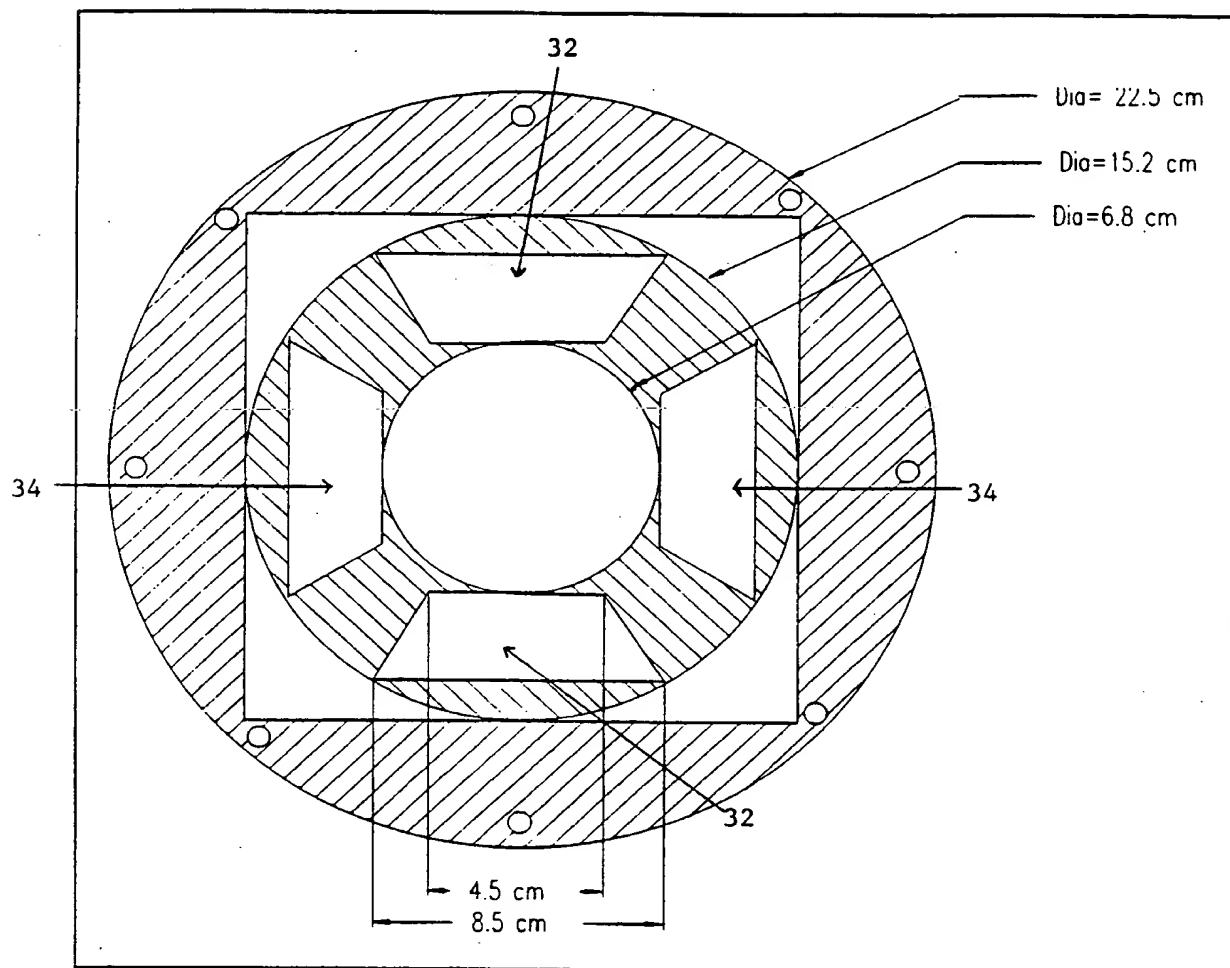


Figure 3 : Cross section of the Venturi, section A-A.

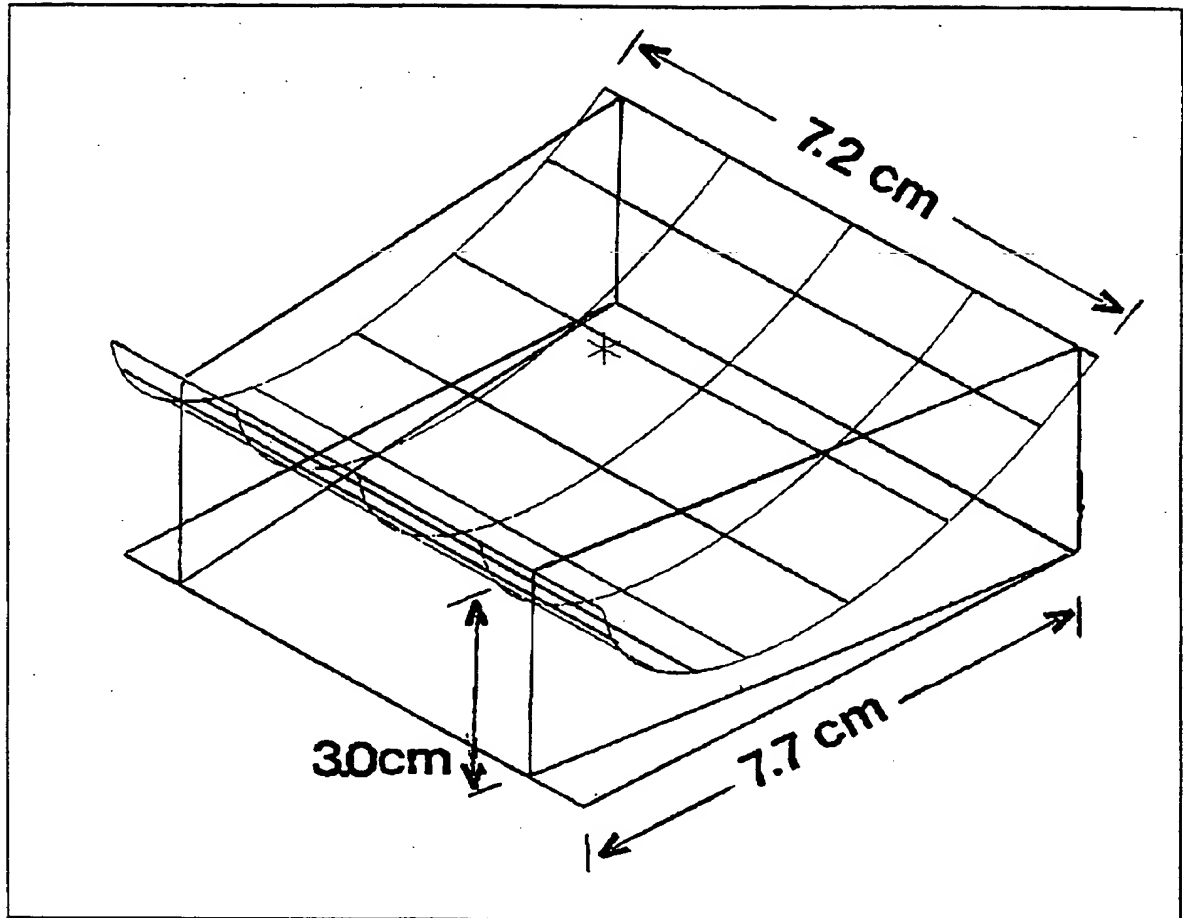
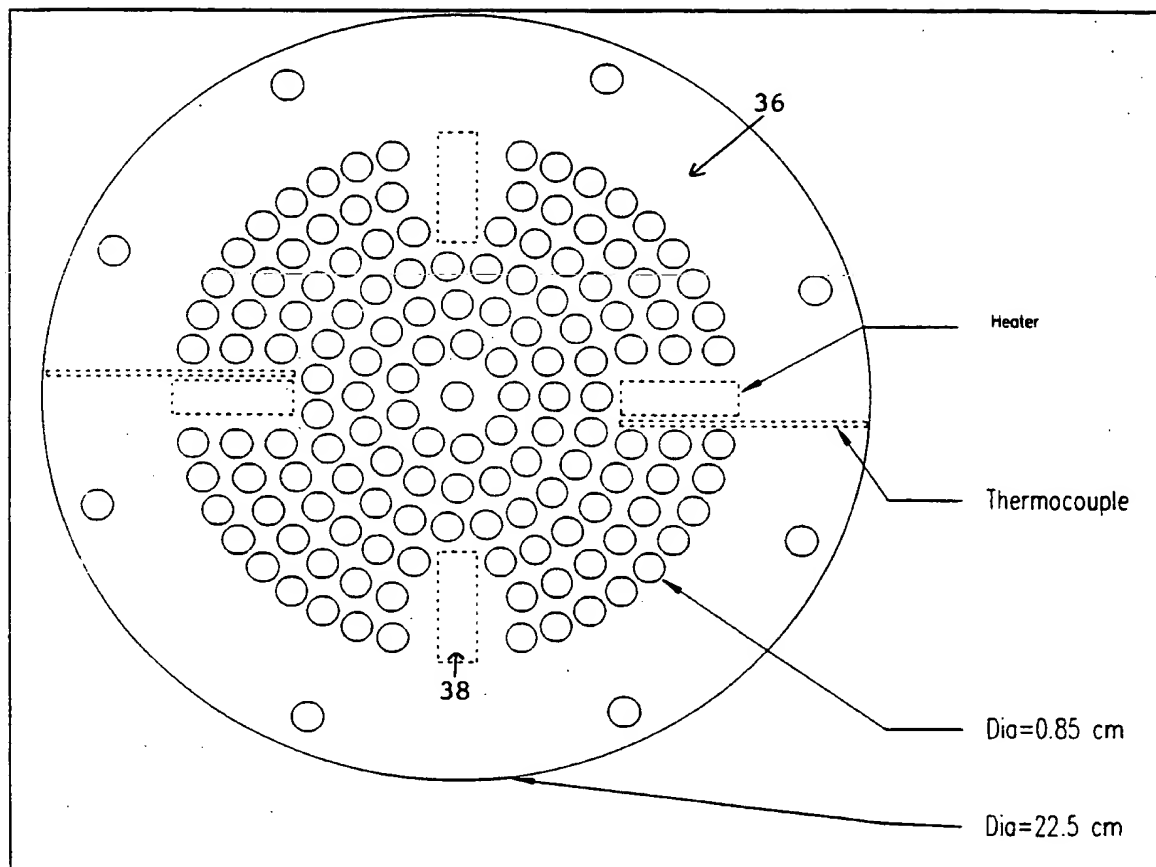


Figure 4 : Details of Photo-CREC-Air reflector.



**Figure 5 : Mechanical drawing of the perforated plate.**

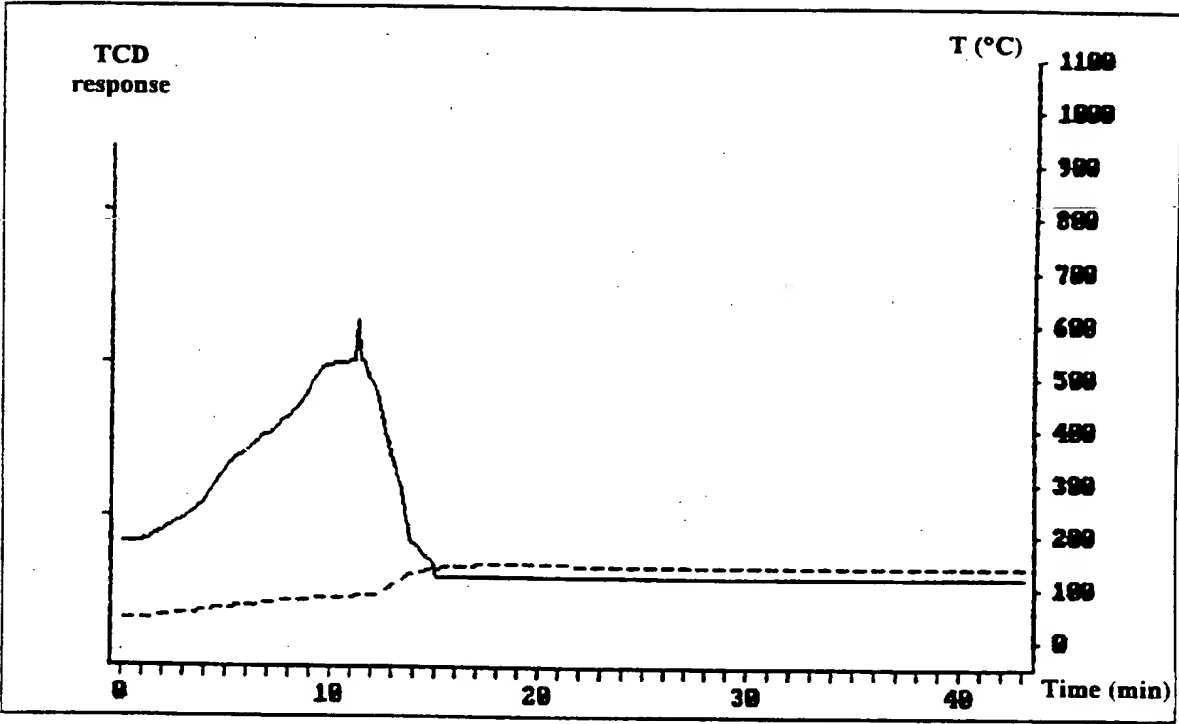


Figure 6: TPD of the 3M Blue Pleated Filter. The full line represents the water desorption from the mesh. The dashed line is the adopted temperature program.

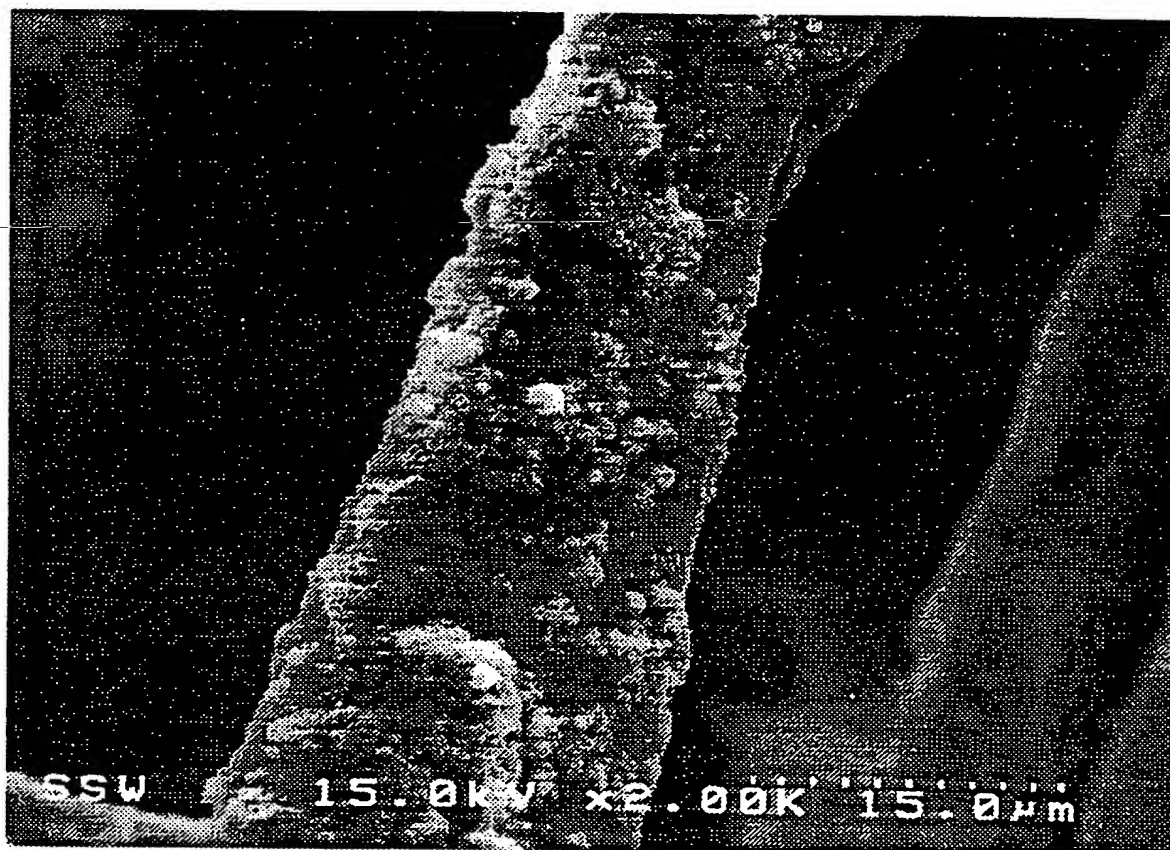


Figure 7 : Close up picture of Figure 5.5 showing a single treated strand and  $\text{TiO}_2$  attached to it firmly.

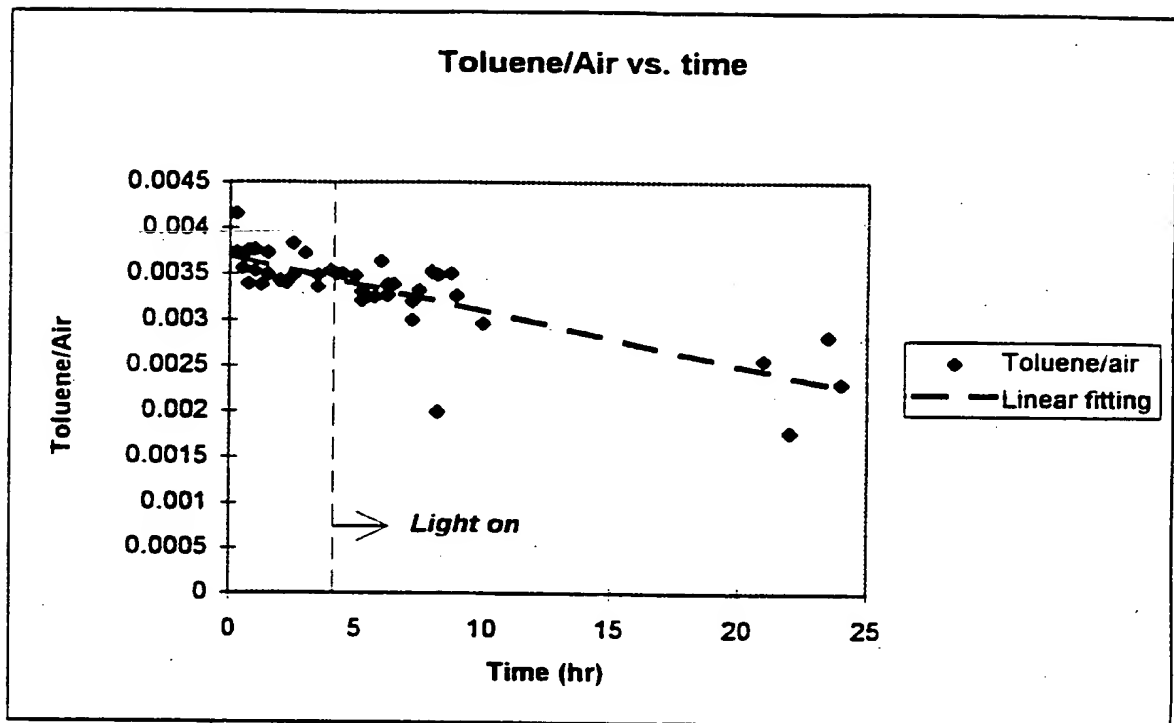


Figure 8 : Toluene/air ratio versus time, the internal standard used in the experimental runs.



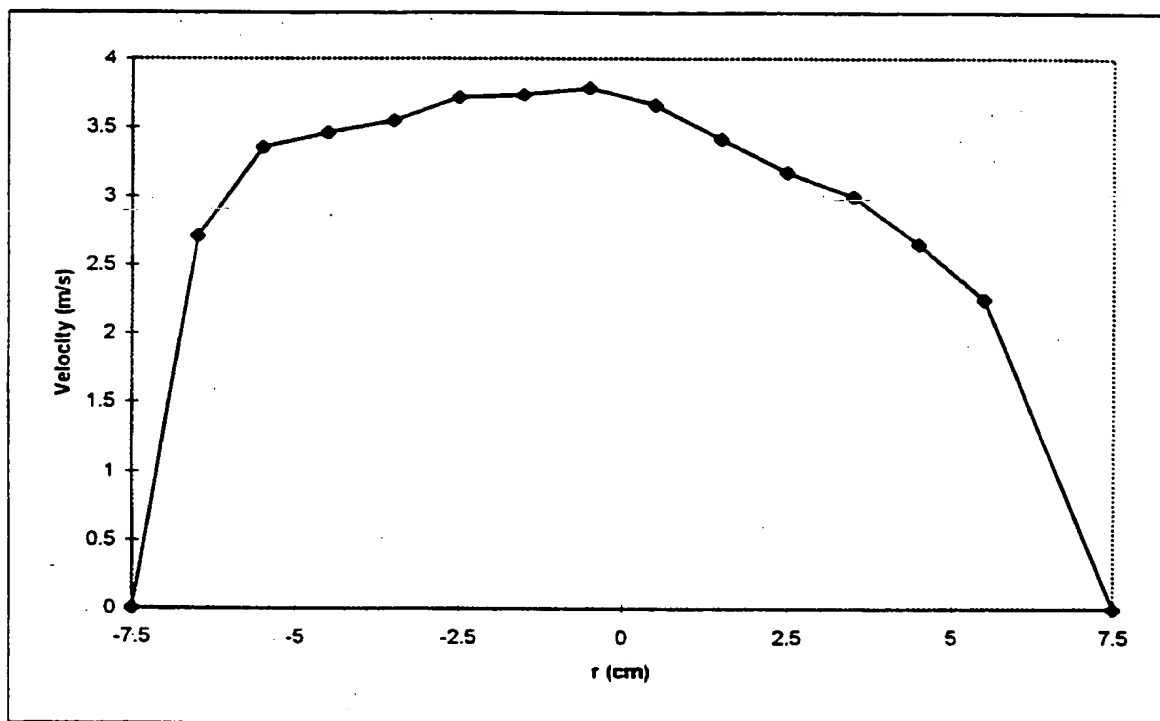


Figure 9A : Velocity profile at 25 °C. Average superficial velocity to 2.83 m/s.

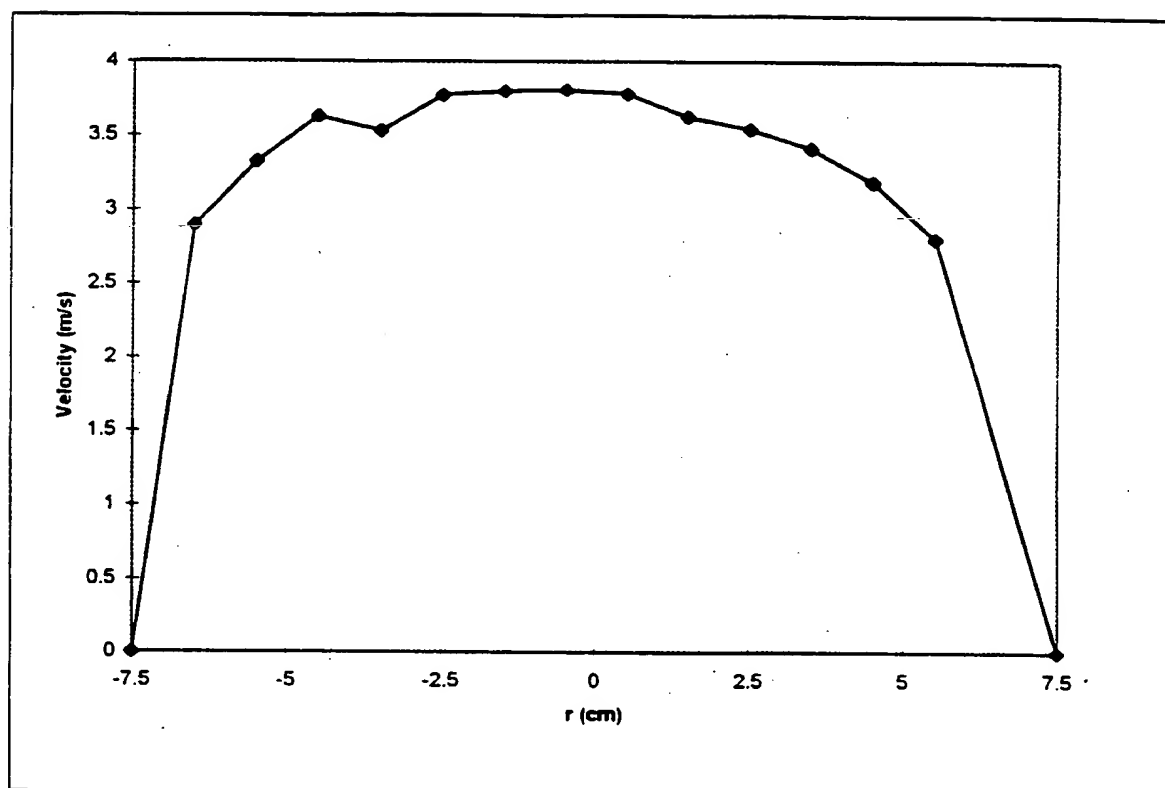


Figure 9B : Average velocity profile at 97°C. Average superficial gas velocity

3.0= m/s.

10/30

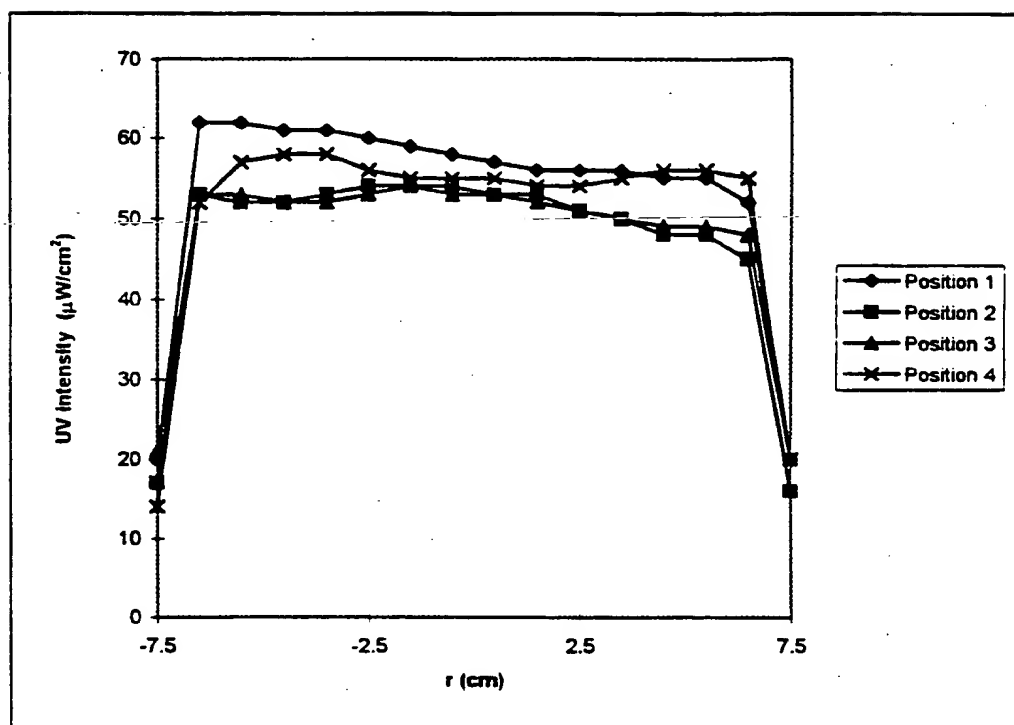


Figure 10A UV intensity profile across the filter sectional area with  $r=0$  representing the center of the filter. Position 1: 0 degrees, Position 2: 90 degrees, Position 3 :180 degrees, Position 4: 270 degrees.

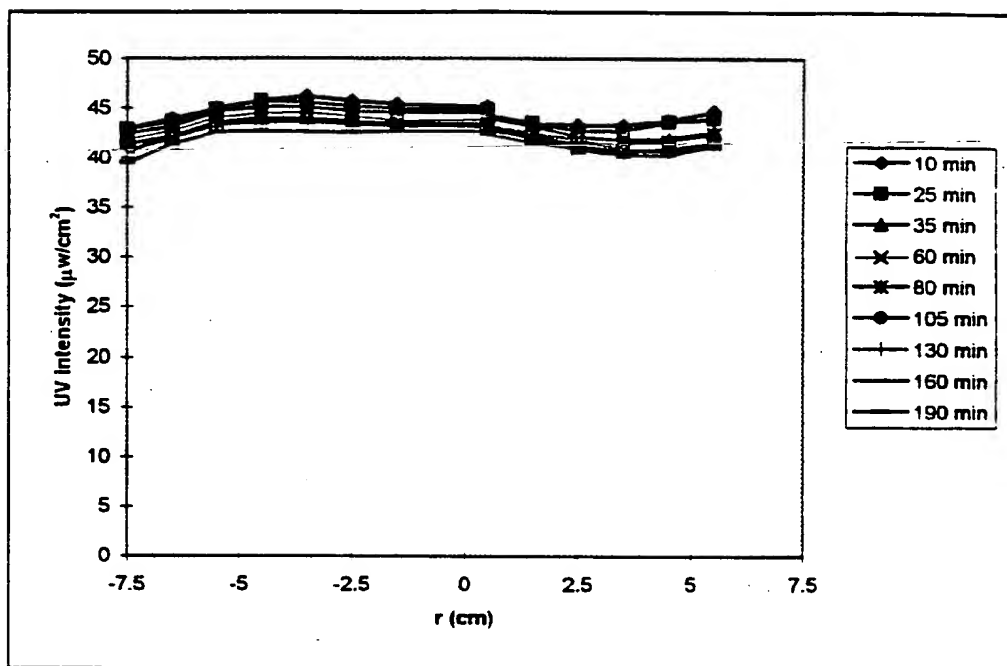


Figure 10B : Radial UV intensity decay profile across the mesh with  $r=0$  representing the center of the mesh.

12/30

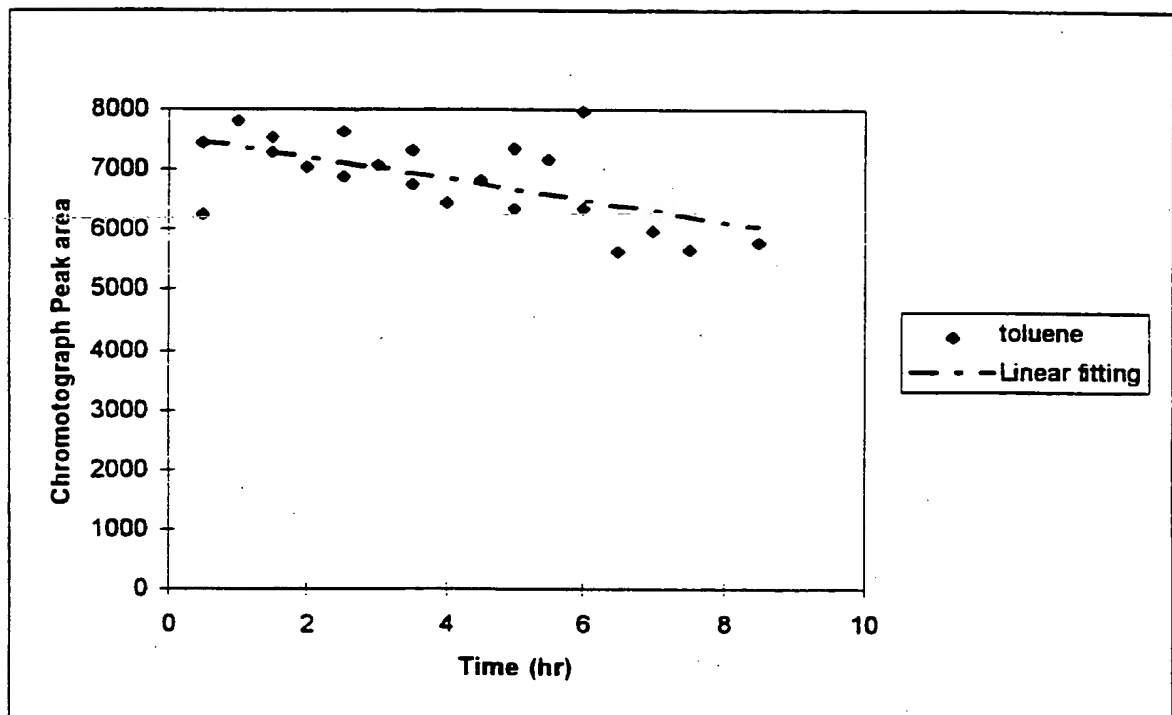


Figure 11A : Results of the blank runs in Photo-CREC-Air lacking  $\text{TiO}_2$  mesh and with no UV irradiation at  $20^\circ\text{C}$ .

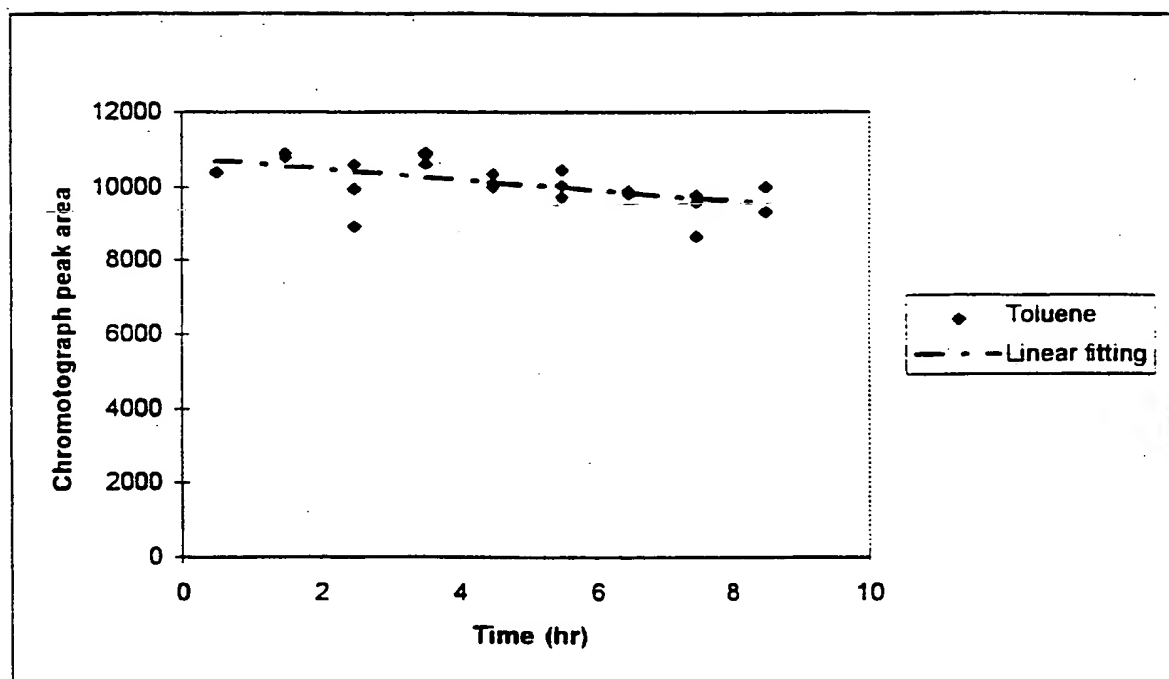


Figure 11B. Results of the blank runs in Photo-CREC-Air lacking  $\text{TiO}_2$  mesh and with no UV irradiation at  $100^\circ\text{C}$ .

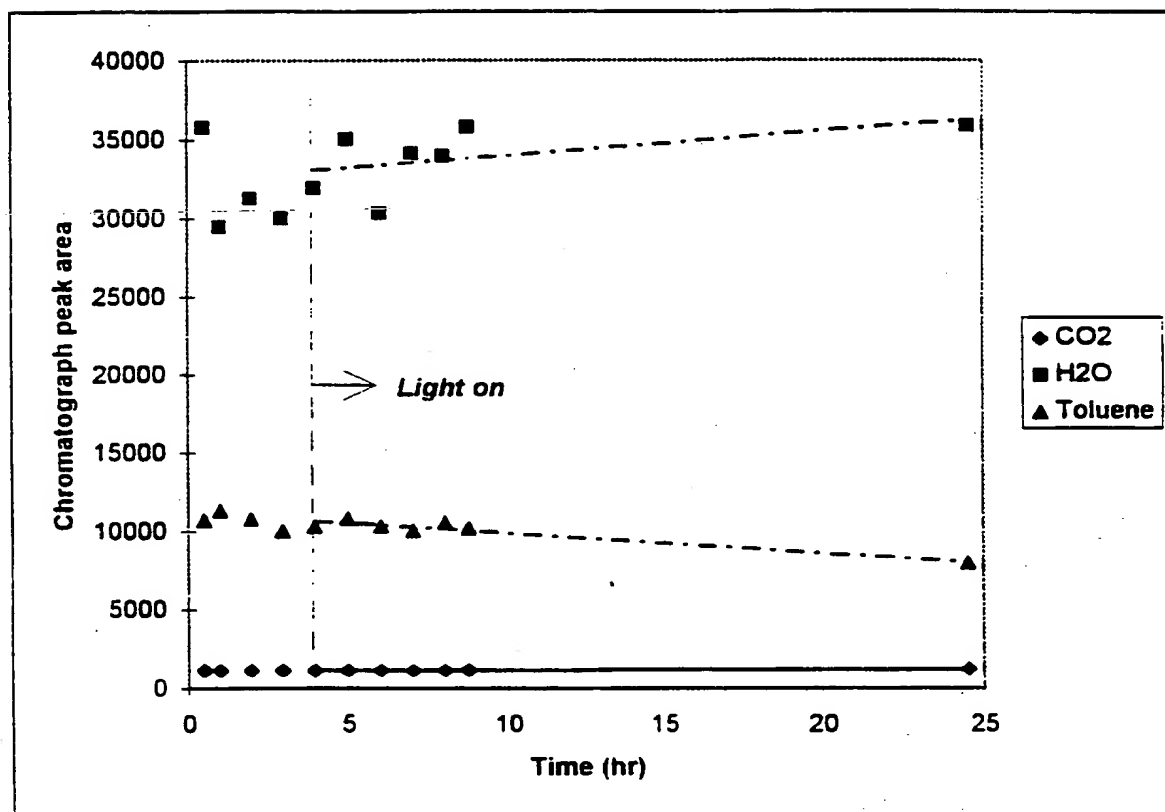


Figure 12 : Typical experimental curves showing changes of reactant and product concentration as a function of time-on-stream with toluene concentration being  $10.4 \mu\text{g}/\text{cm}^3$  and heating plate at  $T=100^\circ\text{C}$ .

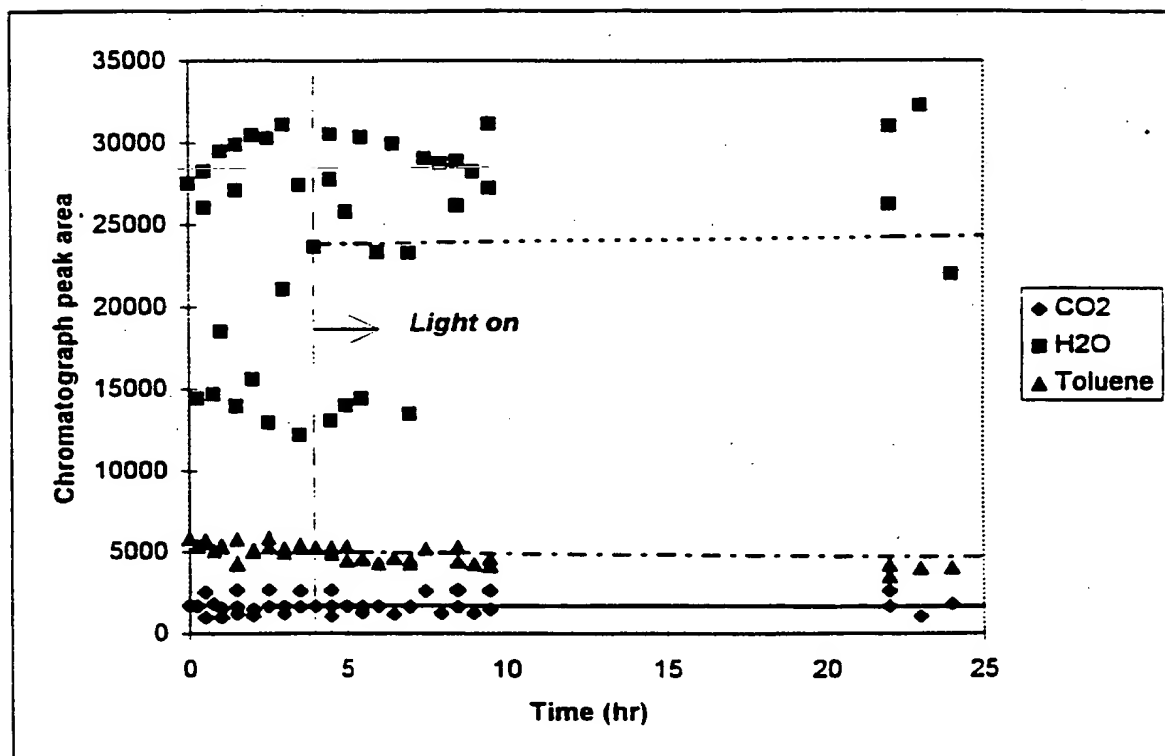


Figure 13A : Experimental run with Photo-CREC-Air: initial toluene concentration=5.2  $\mu\text{g}/\text{cm}^3$ , Temperature=100 °C, water level below 25  $\mu\text{g}/\text{cm}^3$ .



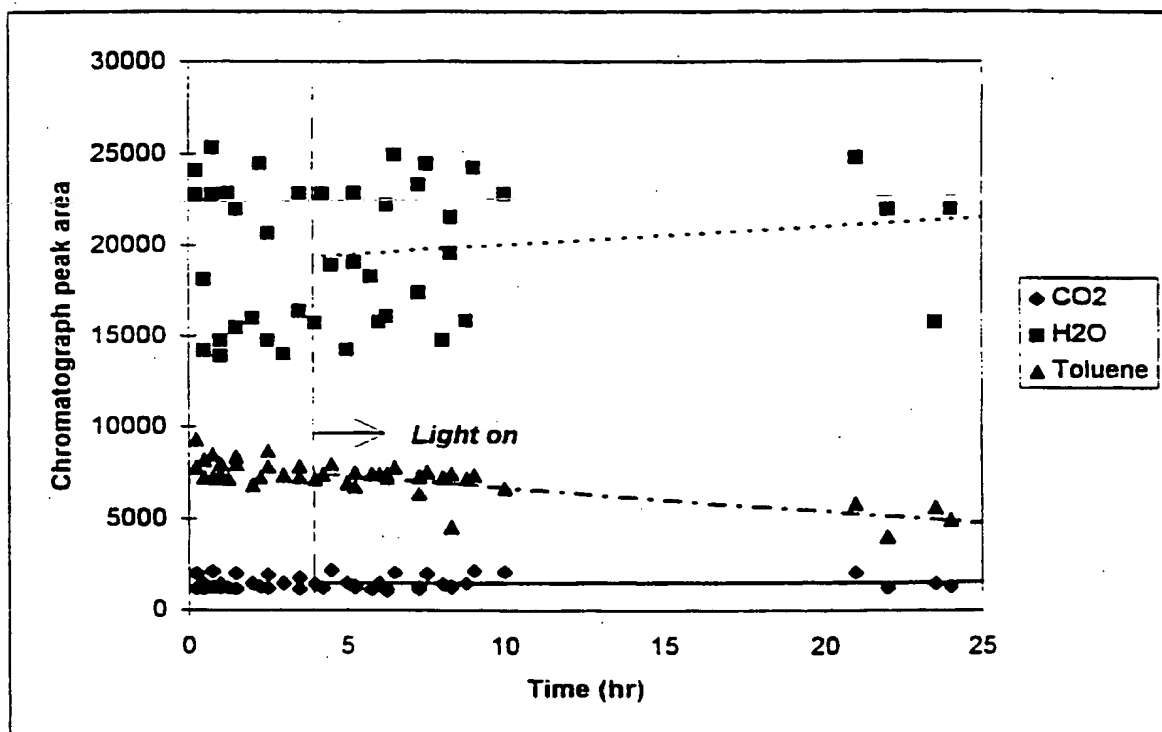


Figure 13B : Experimental run with Photo-CREC-Air: initial toluene concentration= $7.78 \mu\text{g}/\text{cm}^3$ , Temperature= $100^\circ\text{C}$ , water level below  $25 \mu\text{g}/\text{cm}^3$ .

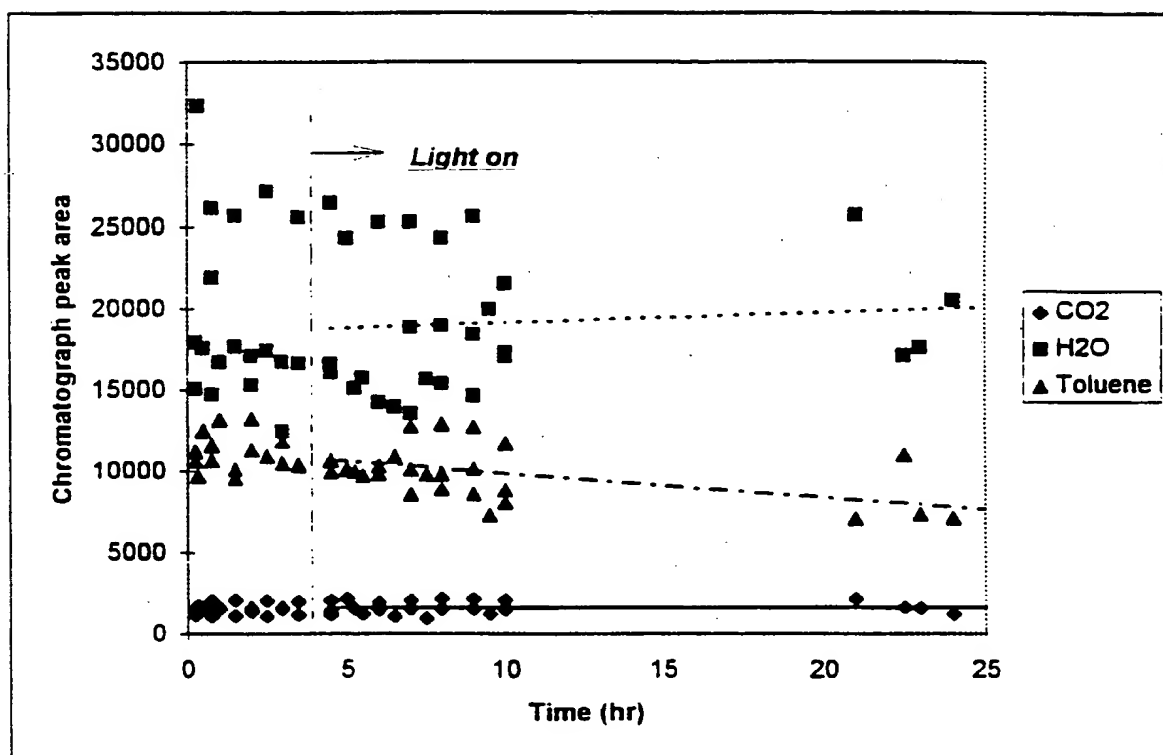


Figure 13B : Experimental run with Photo-CREC-Air: initial toluene concentration= $10.4 \mu\text{g}/\text{cm}^3$ , Temperature= $100^\circ\text{C}$ , water level below  $25 \mu\text{g}/\text{cm}^3$ .

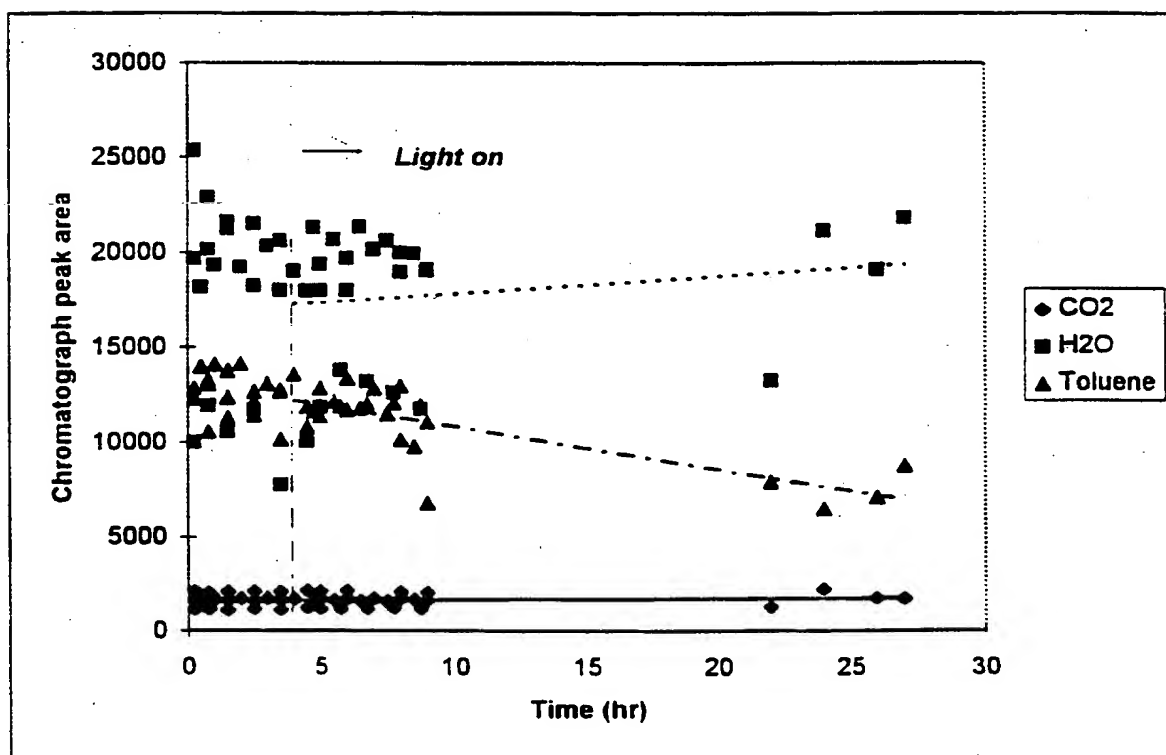


Figure 13D : Experimental run with Photo-CREC-Air: initial toluene concentration= $13 \mu\text{g}/\text{cm}^3$ , Temperature= $100^\circ\text{C}$ , water level below  $25 \mu\text{g}/\text{cm}^3$ .

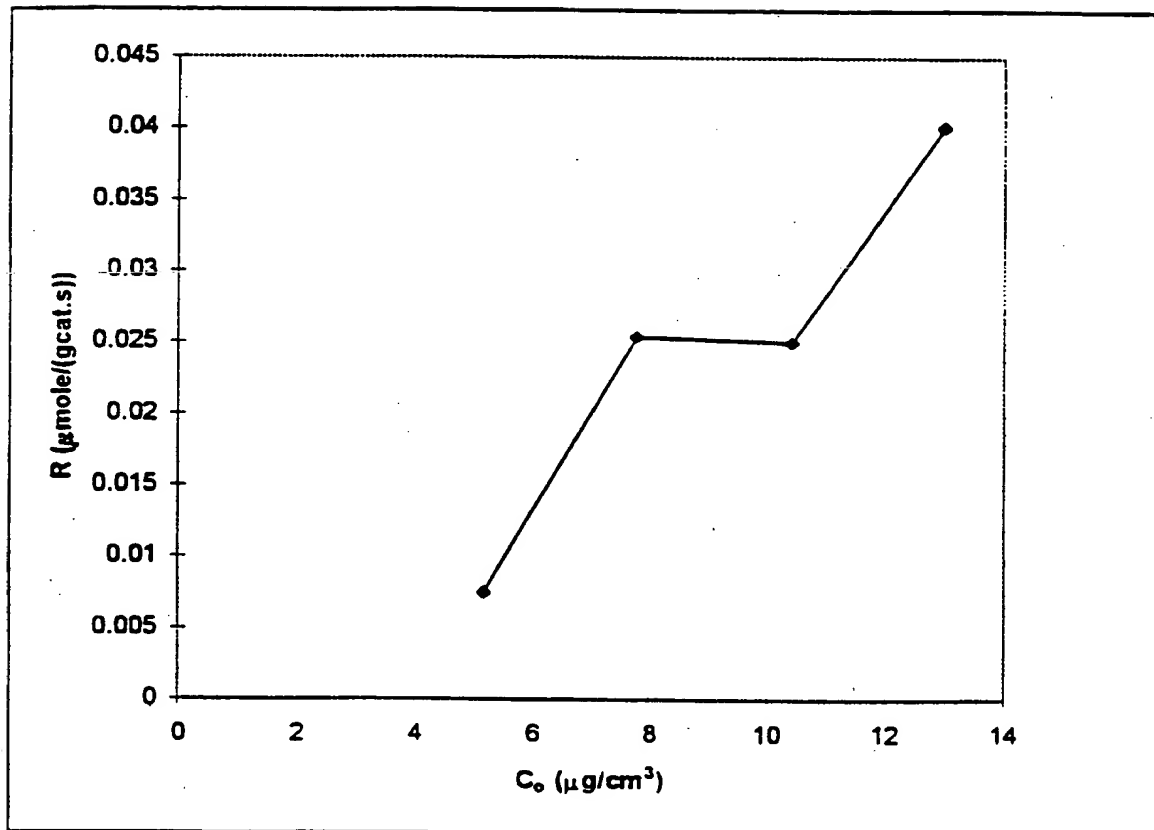


Figure 14 : Rate of toluene oxidation as a function of the initial toluene concentration.

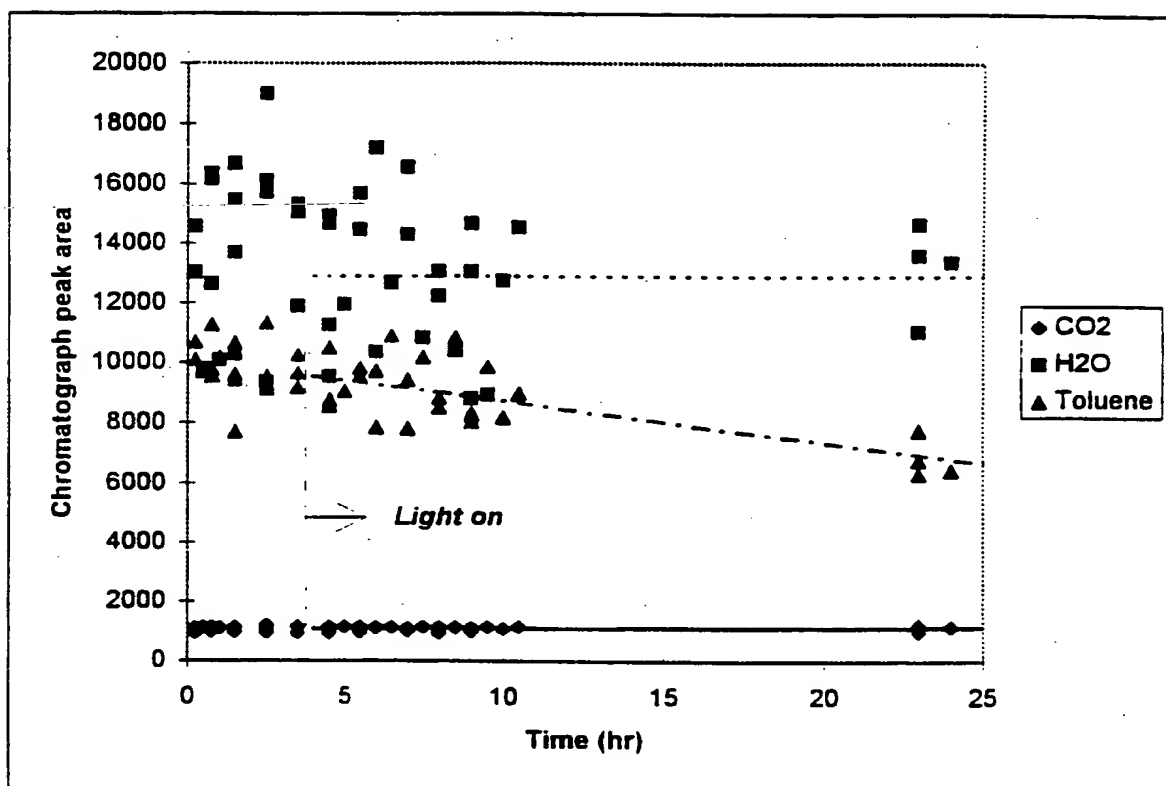


Figure 15A : Experimental run with Photo-CREC-Air: initial toluene concentration= $10.4 \mu\text{g}/\text{cm}^3$ , Temperature= $75^\circ\text{C}$ , water level below  $25 \mu\text{g}/\text{cm}^3$ .

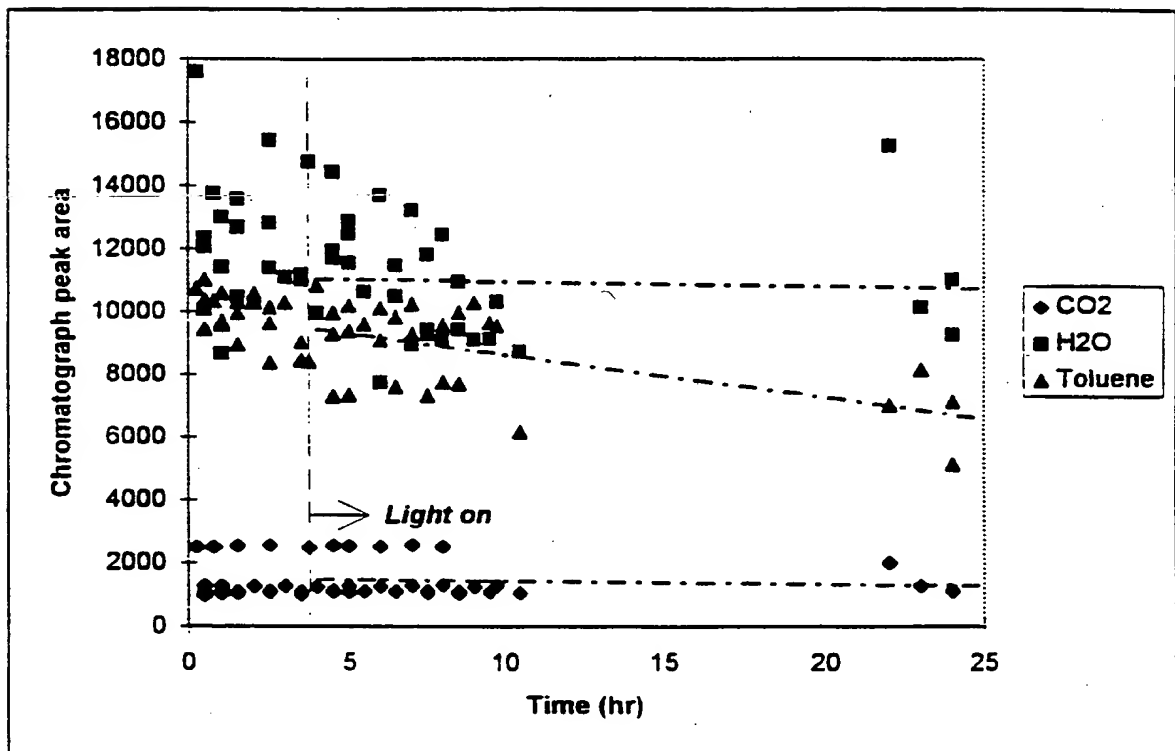
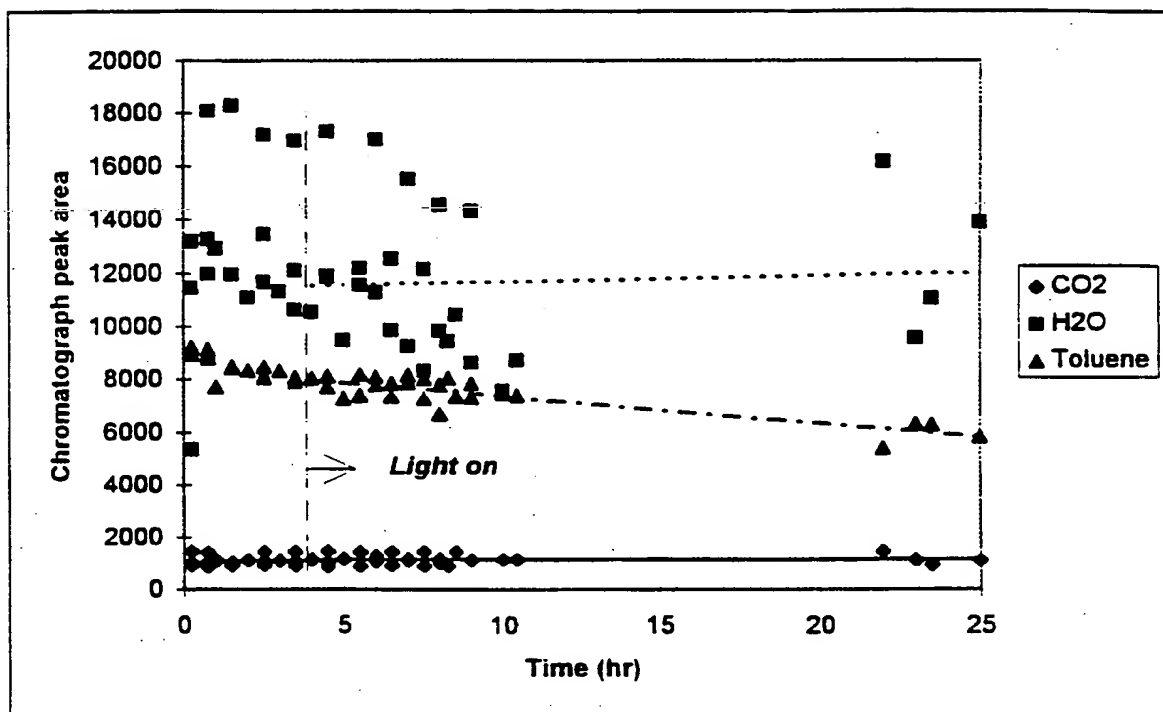


Figure 15B : Experimental run with Photo-CREC-Air: initial toluene concentration=10.4  $\mu\text{g}/\text{cm}^3$ , Temperature=50 °C, water level below 25  $\mu\text{g}/\text{cm}^3$ .



**Figure 15C : Experimental run with Photo-CREC-Air: initial toluene concentration=10.4  $\mu\text{g}/\text{cm}^3$ , Temperature=20  $^{\circ}\text{C}$ , water level below 25  $\mu\text{g}/\text{cm}^3$ .**

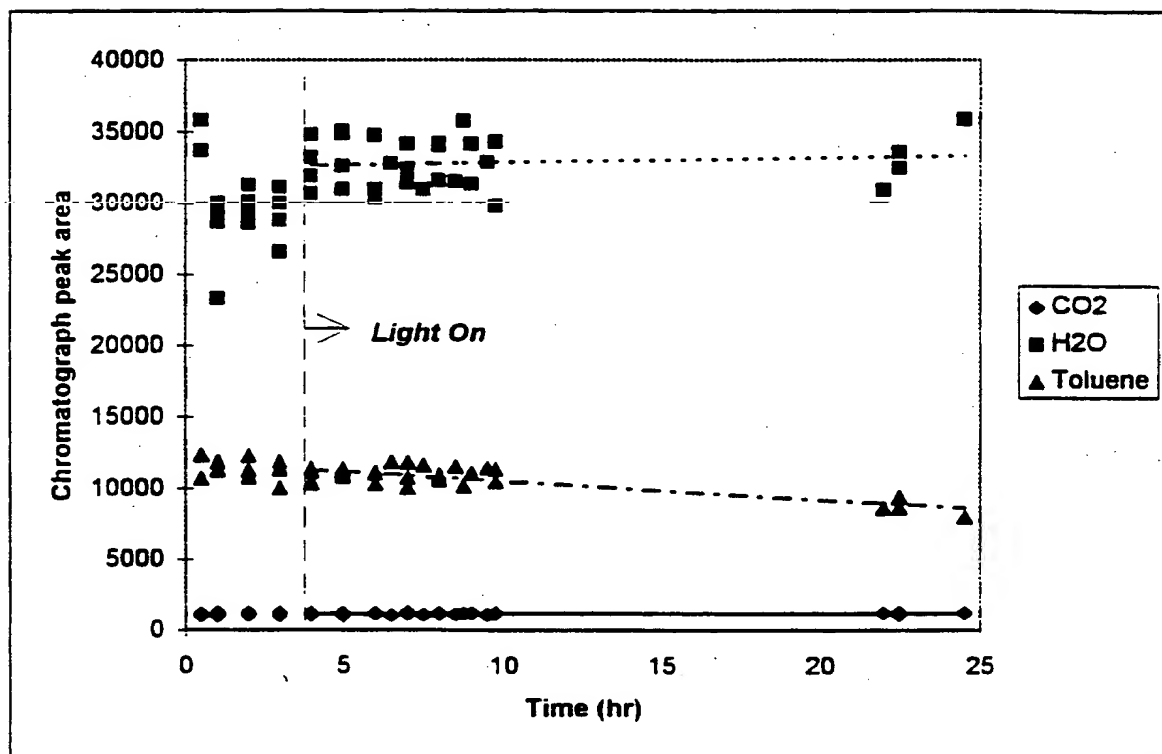


Figure 15D : Experimental run with Photo-CREC-Air: initial toluene concentration= $10.4 \mu\text{g}/\text{cm}^3$ , Temperature= $100^\circ\text{C}$ , water level about  $30 \mu\text{g}/\text{cm}^3$ .



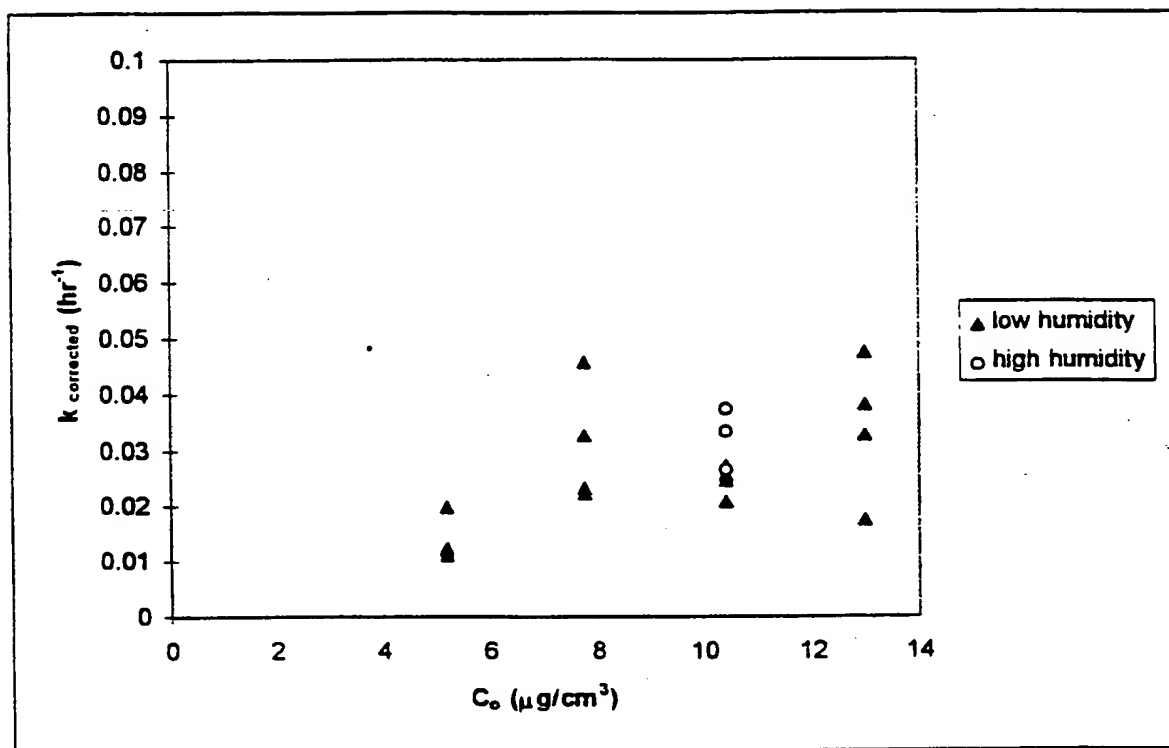


Figure 16A : Kinetic constants for the different initial toluene concentration.

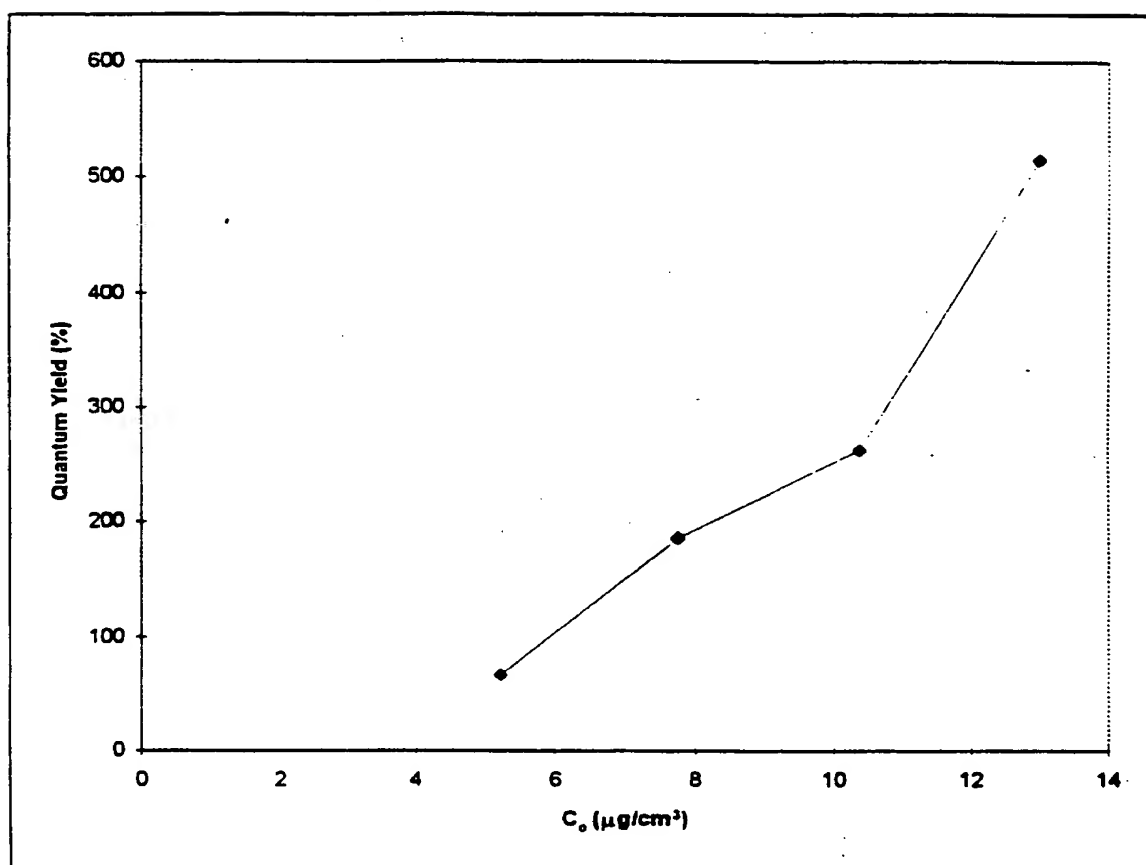


Figure 16B : Quantum yields assessed for the different toluene initial concentrations studied.

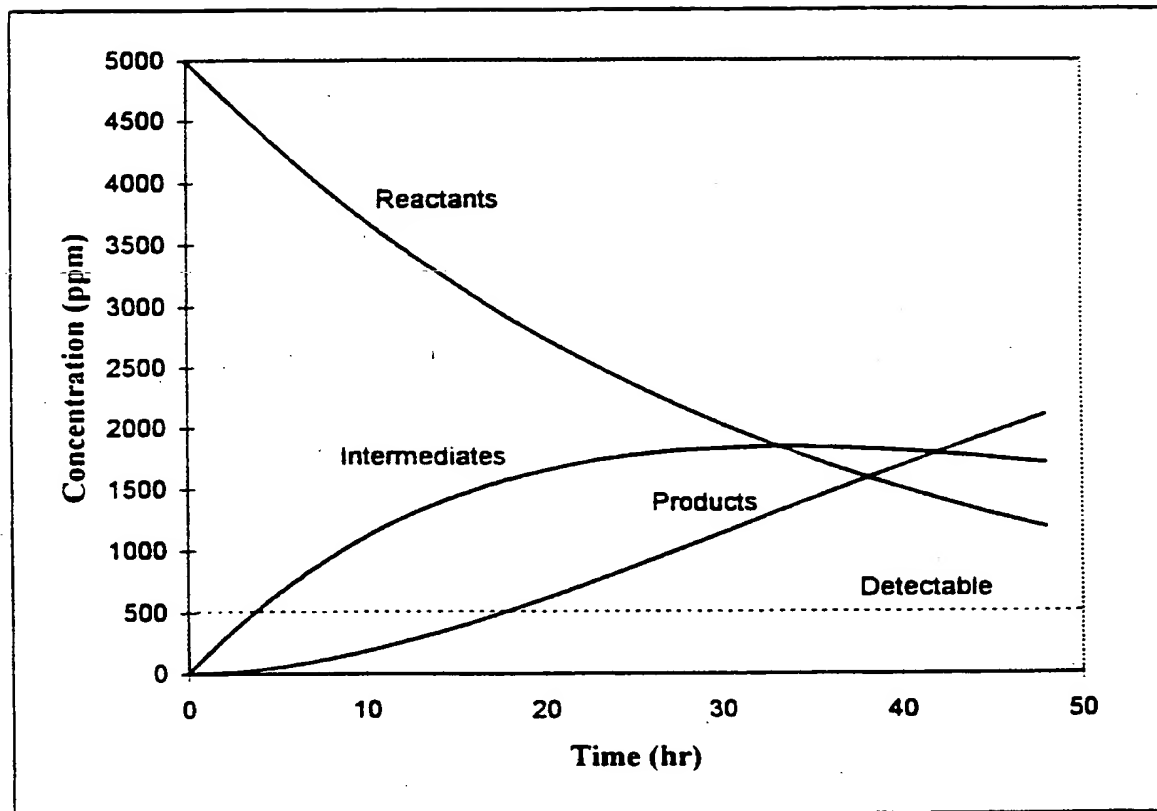


Figure 17A : Simulated chemical species distribution for the following set of constants and operating conditions:  $k_1=0.03(\text{hr}^{-1})$ ,  $k_2=0.03(\text{hr}^{-1})$ , and  $C_o=18 \mu\text{g}/\text{cm}^3$  (5000ppm).

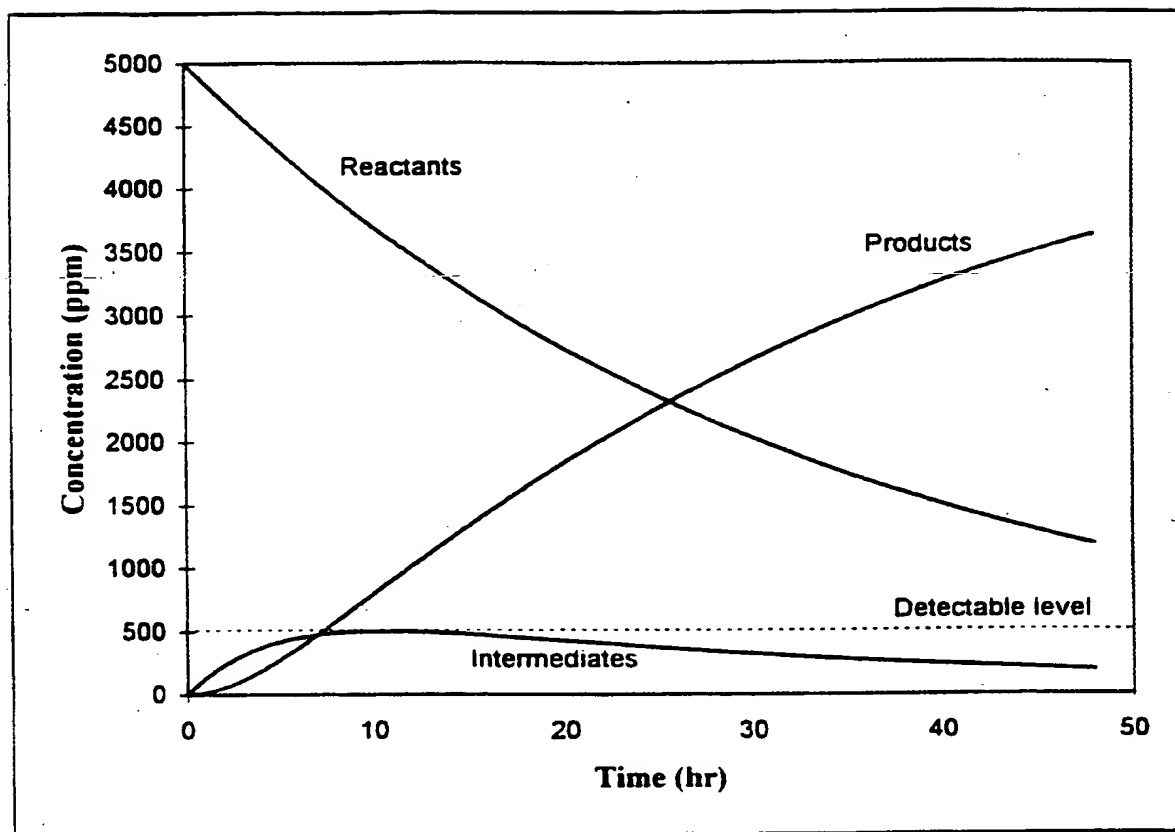


Figure 17B : Simulated chemical species distribution for the following set of constants and operating conditions:  $k_1=0.03 \text{ (hr}^{-1}\text{)}$ ,  $k_2=0.22 \text{ (hr}^{-1}\text{)}$ , and  $C_o= 18\mu\text{g/cm}^3(5000\text{ppm})$ .

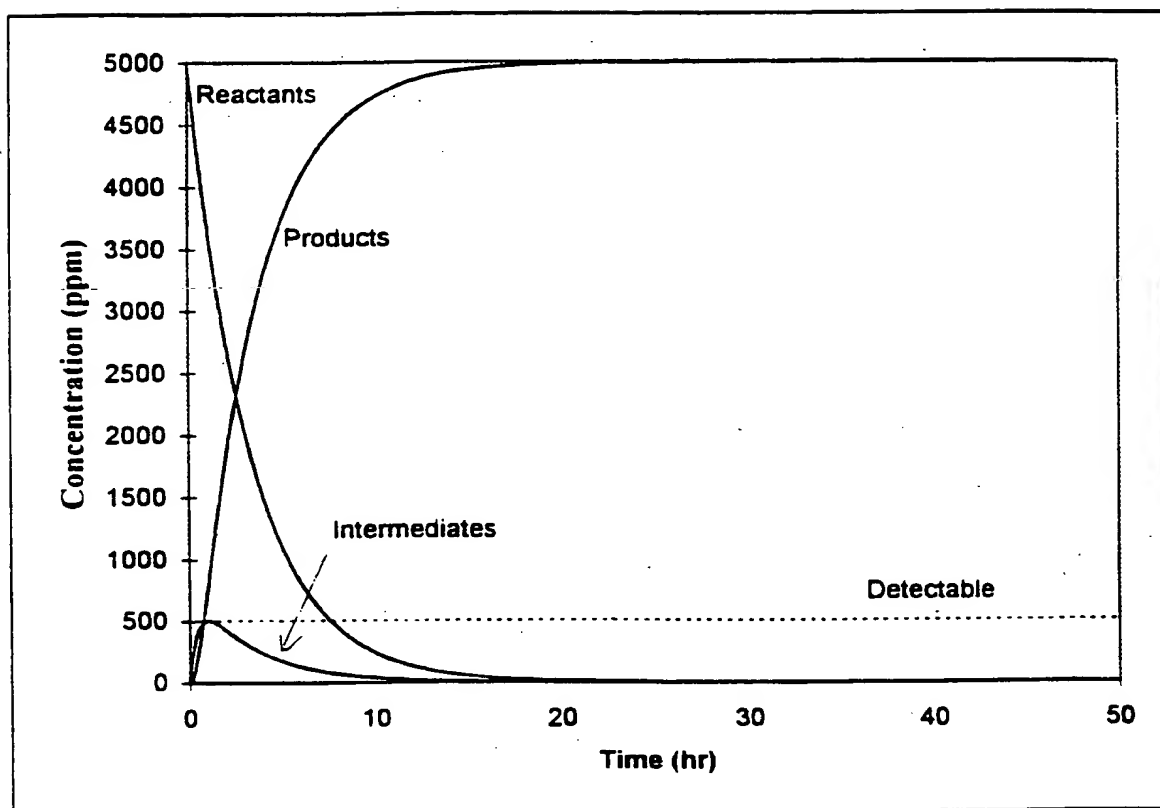


Figure 17C : Simulated chemical species distribution for the following set of constants and operating conditions:  $k_1=0.3 \text{ (hr}^{-1}\text{)}$ ,  $k_2=2.2 \text{ (hr}^{-1}\text{)}$ , and  $C_0=18 \text{ } \mu\text{g/cm}^3\text{(5000ppm)}$ .

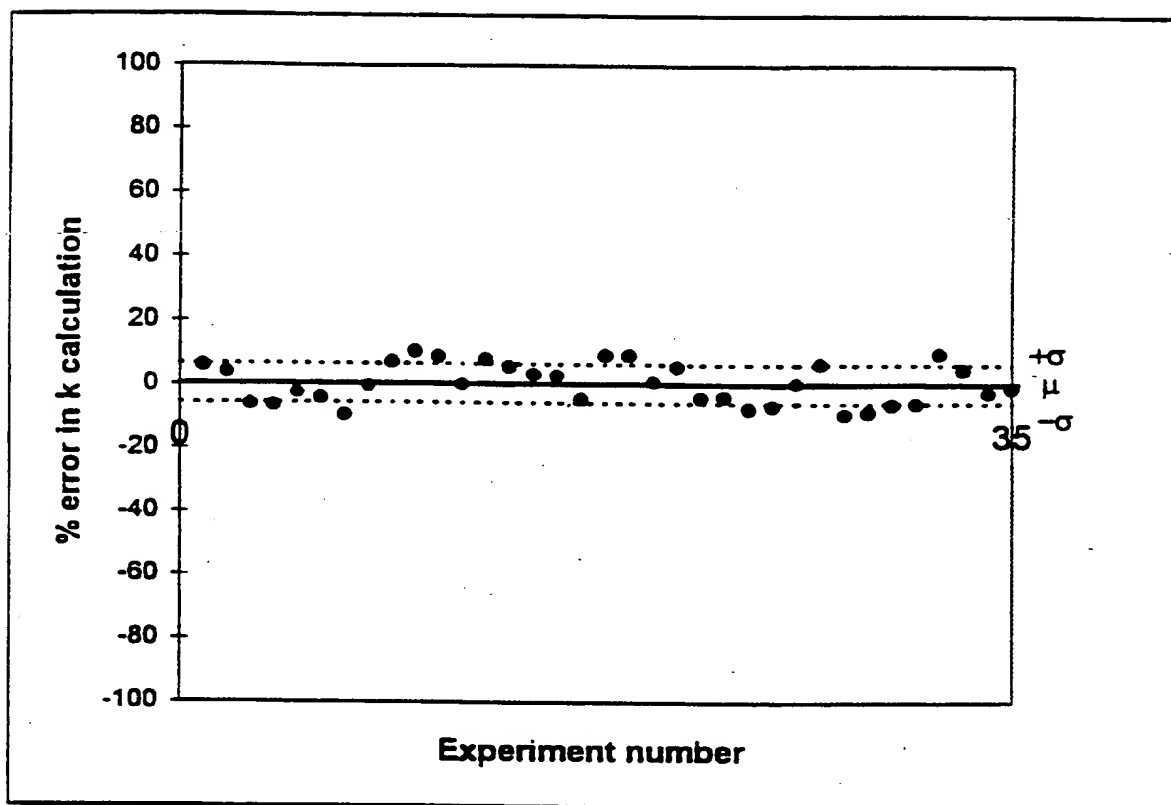


Figure 18 :Estimated errors of the kinetic parameter associated with the different measured variables